ELSEVIER

Journal of Chromatography A, 805 (1998) 71–83

JOURNAL OF CHROMATOGRAPHY A

n-Alkyl fluorenyl phases in chromatography I. Synthesis and characterization

Wolfram Wielandt[a], Arndt Ellwanger[b], Klaus Albert[b], Ekkehard Lindner[a,*]

[a]*Institut für Anorganische Chemie, Auf der Morgenstelle 18, D-72076 Tübingen, Germany*
[b]*Institut für Organische Chemie, Auf der Morgenstelle 18, D-72076 Tübingen, Germany*

Received 24 October 1997; received in revised form 12 December 1997; accepted 31 December 1997

Abstract

A new class of silica gel-bound fluorene phases is described. The compounds are synthesized via reaction of fluorenyl lithium with ω-alkenyl bromides leading to 9-(5′-hexenyl)-9*H*- and 9-(9′-decenyl)-9*H*-fluorene (**1** and **2**), followed by hydrosilation reactions with different hydrosilanes. The resulting ω-functionalized silylalkyl fluorenes **3a(T^0)**, **3b(T^0)**, **4a(T^0)**, **4b(T^0)** and **4c(M^0)** (Scheme 1) react with surface silanol groups of silica gel to generate the new fluorene phases **3a(T^n)(Q^m)$_y$**, **3b(T^n)(Q^m)$_y$**, **4a(T^n)(Q^m)$_y$**, **4b(T^n)(Q^m)$_y$** and **4c(M^1)(Q^m)$_y$**. The phases are characterized by employing ^{1}H, ^{13}C and ^{29}Si solid-state nuclear magnetic resonance spectroscopy. Their applicability in high-performance liquid chromatography is proved by the Sander and Wise test (SRM 869). In contrast to conventional *n*-alkyl phases, π–π interactions are additionally involved in the separation process and, therefore, the retention times of the polycyclic aromatic hydrocarbons sample molecules depend on the ligand densities of the applied fluorene phases. © 1998 Elsevier Science B.V.

Keywords: Stationary phases, LC; Interphases; Solid-state NMR spectroscopy; Nuclear magnetic resonance spectroscopy; Fluorenyl alkyl silanes; π–π interactions; Polynuclear aromatic hydrocarbons

1. Introduction

In environmental analysis, the separation of samples such as polycyclic aromatic hydrocarbons (PAHs) or nitro explosives is an important task. High-performance liquid chromatography (HPLC) is a widespread analytical method for the investigation of environmentally relevant compounds. The proper choice of an optimal stationary phase is essential for a successful HPLC separation. A typical stationary phase consists of a polymeric backbone, which is mostly modified with different organic ligand fragments. Silica gel is often used as a matrix material, because it has well-defined surface silanol groups that can easily be modified by organosilanes and it is insoluble under normal chromatographic conditions. For the HPLC separation of aromatic sample mixtures, two different kinds of stationary phases can be applied. The conventional separation technique uses *n*-alkyl-bound stationary phases, mostly C_{18} phases [1,2], whereas recently described separations have been performed using stationary phases with aromatic ligand fragments, such as anthracene, acridine [3–9] and fluorene [10–12]. When using aromatic ligand fragments, the aromatic moiety was connected to silica gel by amido couplings with spacers of

*Corresponding author.

0021-9673/98/$19.00
PII S0021-9673(98)00014-4

aminoalkyl silanes and glutaric acid. Hydrophobic interactions between the alkyl chains, the solvent and the solute molecules are responsible for the separation in the case of the *n*-alkyl phases, in which the alkyl chains are both the main interaction center and the spacer attached to the surface of the silica gel in one functionality. For aromatic phases, the aromatic ligand fragments are the main interaction centers and π–π interactions with the solute molecules predominate [13,14]. The spacer units are chemically different with respect to the main interaction center and, because of their deficiency of π-electrons, their contribution to the interaction process is limited. These systems, in which a mobile phase penetrates a stationary phase consisting of a matrix, a spacer and an active center, are called ''interphases'' [15,16], because the solvent is able to solvate the organic ligand fragments and, therefore, improve their interaction ability by increasing their mobility.

The concept of interphases is not only limited to chromatographic techniques like HPLC. It has also been applied in fields such as catalysis, combining the advantages of homogeneous catalysis with those of heterogeneous catalysis [17–22]. In an analogous manner to that in chromatography, a transition metal complex is connected to the matrix by a spacer and the solvent is able to solvate the reactive center and the spacers. Thus, no homogeneous mixture is formed and the catalyst can be easily removed from the reacted substrate. In catalysis, the functionality is denoted as a reactive center, in chromatography however, it is called the interaction center. The activities and selectivities obtained by these types of transition metal catalysts are strongly influenced by their mobility. It has been shown that a higher mobility of the spacer increases that of the catalytic system, and conclusively leads to an increasing turnover number and improved selectivity [19–22].

The common aim of both techniques, i.e. chromatography and catalysis, is to increase the effectiveness of the interaction and reactive centers, respectively, by optimising the system's mobility.

In recent investigations, Brindle and Albert [10] were able to demonstrate the chromatographic capability of fluorene phases for separations of both PAHs and nitro explosives. The predominance of π–π interactions during the separation process could be proved by comparing the drastically changed elution order of nitro explosives attained by the use of either a fluorene or a C_{18} stationary phase [23,24]. An increasing number of nitro groups attached to the aromatic solute molecule resulted in an increasing π-electron acceptor activity. The corresponding nitro compound separation behavior entailed increased retention, because stable donor–acceptor complexes of the nitro compounds with the fluorene ligands of the stationary phase, acting as π-electron donors, were formed. The influence of the pore size of the silica gel on the separation efficiency was also studied. The best results were achieved with silica gel with a pore size of 200 Å. Due to a weaker curvature of the pores, the packing density of the terminal fluorene ligands was lower and their mobility increased. Therefore, the separation efficiency of the interphase was much better for larger solute molecules, because easier diffusion into the stationary phase resulted in a more effective interaction.

Although the mobility of the fluorene ligands could be improved by using silica gel with a larger pore size, the described fluorene phase was still rather immobile, because of the influence of the spacer, which consisted of aminopropylsilane and glutaric acid. Partial double bonds of the C–N groups reduced the mobility of the whole spacer and, hence, also that of the fluorene ligand fragments.

Therefore, our intention was to further improve the overall mobility of the interaction center of the stationary phase by connecting fluorene to silica gel with an *n*-alkyl chain. In this paper, we describe first the synthesis of different fluorenyl alkyl silanes, which differ in the length of their *n*-alkyl chain, and in the type and the functionality of the hydrosilane. In a further step, these fluorenyl alkyl silanes are immobilized on silica gel to obtain new stationary phases for HPLC. Secondly, we characterize the structure of the new developed stationary phases by solid-state nuclear magnetic resonance (NMR) spectroscopy [25]. ^{29}Si CP/MAS (cross polarization/magic angle spinning) NMR spectroscopy provides information about the surface of the chemically modified silica gel, whereas information about the different organic ligand fragments is obtained by ^{13}C CP/MAS and ^{1}H MAS NMR spectroscopy. Finally, the utility of the new fluorene phases for HPLC separations is demonstrated by application of a test mixture. We decided to apply the Sander and Wise

test (SRM 869) [26,27], because it contains three different PAHs that should easily be separable by π–π interactions. This test is widely accepted for the characterization of *n*-alkyl stationary phases. The HPLC results are correlated with the different synthetic conditions and the ligand density of the respective stationary phase.

2. Experimental

2.1. General procedures

The synthesis of the alkenyl fluorenes, **1** and **2**, was performed under argon using the usual Schlenk techniques. Diethyl ether, diisopropyl ether and tetrahydrofuran (THF) were distilled from sodium benzophenone ketyl and stored under argon. $HSiCl_3$ and $HSiCl_2(CH_3)$ were stored under argon; all other silanes were used as received from commercial sources. The elemental analyses of carbon and hydrogen were carried out on a Carlo Erba analyzer, model 1106. Chlorine was determined by the method of Schöniger [28,29]. EI mass spectra were recorded on a Finnigan TSQ 70 instrument, and FD mass spectra on a Finnigan MAT 711 A instrument (8 kV, 333 K), modified by AMD (Harpstedt, Germany). NMR spectra in solution ($CDCl_3$) were measured in 5 mm sample tubes on a Bruker DRX 250 NMR spectrometer ($^{13}C\{^1H\}$NMR: 62.9 MHz, internal standard, tetramethylsilane (TMS), 300 K; ^1H NMR: 250.13 MHz, internal standard, TMS, 300 K).

^{29}Si solid-state NMR spectra were obtained on a Bruker MSL 200 NMR spectrometer at 4.7 T. The samples were packed into double bearing 7 mm rotors of ZrO_2, which were spun at 3000 Hz by a dry air gas drive. The proton 90 degree pulse length was 5.5 μs, the recycle delay was 1 s and the contact time was 5 ms. ^{13}C- and ^1H-solid-state NMR spectra were obtained on a Bruker ASX 300 NMR spectrometer at 7 T. For ^1H NMR measurements, 4 mm rotors were spun at 14 kHz, the recycle delay was 4 s and the 90 degree pulse length was 3.8 μs. ^{13}C NMR measurements were also carried out with 4 mm rotors, but the spinning speed was 10 kHz, with a proton 90 degree pulse length of 3.8 μs, a contact time of 1 ms and a recycle delay of 1 s. All chemical shifts were externally referenced to liquid tetramethylsilane. The Hartmann-Hahn condition for CP was calibrated with glycine (^{13}C) or Q_8M_8 (^{29}Si).

2.2. Chromatography

HPLC separations were performed with a Merck/Hitachi L-6200 A pump and a variable wavelength detector (Merck/Hitachi L-4000 A; Merck–Hitachi, Darmstadt, Germany). The stationary phases were packed into 250×4 mm stainless steel tubes (Bischoff, Leonberg, Germany) by a high pressure slurry packing procedure on a Knauer Pneumatic HPLC pump (Knauer, Berlin, Germany). The mobile phase comprised a mixture of acetonitrile–water (85:15, v/v). The wavelength used for UV detection was 254 nm, the flow-rate was 1 ml/min and the temperature was maintained at 25°C. A 10-μl volume of the SRM 869 test sample was injected each time.

2.3. Materials

1-Bromo-5-hexene and 1-bromo-9-decene were synthesized according to methods described in the literature [30,31]. The corresponding alcohols were purchased from Merck-Schuchardt (Hohenbrunn, Germany). Fluorene, *n*-butyl lithium (15% solution in *n*-hexane) and acetonitrile (gradient grade for HPLC) were from Merck (Darmstadt, Germany), chlorodimethylsilane and triethoxysilane were from Fluka (Buchs, Switzerland), and trichlorosilane and dichloromethylsilane were obtained from Wacker (Burghausen, Germany). The silica gels used were Prontosil 200 Å, 5 μm (surface area 200 m^2/g) from Bischoff and 200 Å, 5 μm silica gel (surface area 200 m^2/g) from YMC Europe (Scharmbeck, Germany). Prontosil was used for the preparation of all of the stationary phases, with the exception of **3b(T^n)(Q^m)$_y$**. In this case, silica gel from YMC Europe was used.

The NIST SRM 869 test mixture was a gift from the National Institute of Standards and Technology (Gaithersburg, MD, USA).

2.4. 9-(5′-Hexenyl)-9H-fluorene (*1*)

To a solution containing 16.62 g (100.0 mmol) of

fluorene in 450 ml of diethyl ether, a 1.6 *M* solution of *n*-butyl lithium in *n*-hexane (62.5 ml, 100.0 mmol) was added dropwise at 0°C. After warming to room temperature, the reddish–brown solution was stirred for 1 h. At 0°C, 17.94 g (110.0 mmol) of 1-bromo-5-hexene were added, and the mixture was stirred for 24 h. After hydrolysis with 100 ml of a 0.2 *M* mixture of NaH_2PO_4–Na_2HPO_4, the resulting two phases were separated, the aqueous phase was washed with 100 ml of diethyl ether and the combined organic phases were dried over sodium sulfate. The solvent was removed in vacuo and the residual oil was purified on a silica gel column using toluene as the eluting solvent, giving a yield of 21.9 g (88.2%).

MS (EI) *m/e* 248.2 [M^+, 10], 178.0 [M^+–C_5H_{10}, 37], 165.0 [M^+–C_6H_{11}, 58], 91.1 [$C_7H_7^+$, 100], 83.2 [$C_6H_{11}^+$, 67], 55.1 [$C_4H_7^+$, 81]. Analytical results: Found: C, 91.80; H, 8.13. $C_{19}H_{20}$. Calculated: C, 91.88; H, 8.12. $^{13}C\{^1H\}$ NMR (62.90 MHz, $CDCl_3$, 300 K): δ 25.0 (C^{11}; for labeling of the carbon atoms, see Fig. 1), 29.1 (C^{12}), 32.7 (C^{10}), 33.4 (C^{13}), 47.3 (C^9), 114.2 (C^{15}), 119.7 (C^4, C^5), 124.1 (C^1, C^8), 126.6 (C^2, C^7), 126.7 (C^3, C^6), 138.6 (C^{14}), 141.0 (C^{4a}, C^{5a}), 147.3 (C^{8a}, C^{9a}); ^1H NMR (250.13 MHz, $CDCl_3$, 300 K): δ 7.95 (d, ^2J=6.6 Hz, 2H, C^1H, C^8H), 7.71 (d, ^2J=6.9 Hz, 2H, C^4H, C^5H), 7.54 (m, 4H, C^2H, C^3H, C^6H, C^7H), 5.96 (m, 1H, $C^{14}H$), 5.20 (m, 2H, $C^{15}H_2$), 4.16 (t, ^2J=5.8 Hz, 1H, C^9H), 2.21 (m, 4H, $C^{10}H_2$, $C^{13}H_2$), 1.58 (m, 2H, $C^{12}H_2$), 1.47 (m, 2H, $C^{11}H_2$).

*2.5. 9-(9′-Decenyl)-9H-fluorene (**2**)*

Compound **2** was synthesized in diisopropyl ether in the same way as for **1**: In 300 ml of diisopropyl ether, 15.79 g (95.0 mmol) of fluorene were treated with 59.4 ml of a 1.6-*M* solution of *n*-butyl lithium in *n*-hexane (95.0 mmol). Then, 22.0 g (100.0 mmol) of 1-bromo-9-decene were slowly dropped into the brown solution, and the mixture turned orange. Further steps were performed as described in Section 2.4 to yield 24.6 g (85.1%) of compound **2**.

MS (EI) *m/e* 304.4 [M^+, 5], 178.0 [M^+–C_9H_{18}, 42], 164.9 [M^+–$C_{10}H_{19}$, 100], 69.1 [$C_5H_9^+$, 25], 54.4 [$C_4H_7^+$, 71], 41.0 [$C_3H_5^+$, 82]. Analytical results. Found: C, 90.57; H, 9.14. $C_{23}H_{28}$. Calculated: C, 90.73; H, 9.27. $^{13}C\{^1H\}$ NMR (62.90 MHz, $CDCl_3$, 300 K): δ 25.6 (C^{11}), 28.8 (C^{16}), 29.0 (C^{13}), 29.3 (C^{12}), 29.4 (C^{15}), 29.9 (C^{14}), 33.0 (C^{17}), 33.8 (C^{10}), 47.4 (C^9), 114.1 (C^{19}), 119.7 (C^4, C^5), 124.2 (C^1, C^8), 126.7 (C^2, C^3, C^6, C^7), 139.0 (C^{18}), 141.0 (C^{4a}, C^{5a}), 147.5 (C^{8a}, C^{9a}); ^1H NMR (250.13 MHz, $CDCl_3$, 300 K): δ 7.88 (d, ^2J=6.6 Hz, 2H, C^1H, C^8H), 7.64 (d, ^2J=6.9 Hz, 2H, C^4H, C^5H), 7.46 (m, 4H, C^2H, C^3H, C^6H, C^7H), 5.99 (m, 1H, $C^{18}H$), 5.17 (m, 2H, $C^{19}H_2$), 4.10 (t, ^2J=5.8 Hz, 1H, C^9H), 2.17 (m, 4H, $C^{10}H_2$, $C^{17}H_2$), 1.39 (m, 12H, $C^{11}H_2$–$C^{16}H_2$).

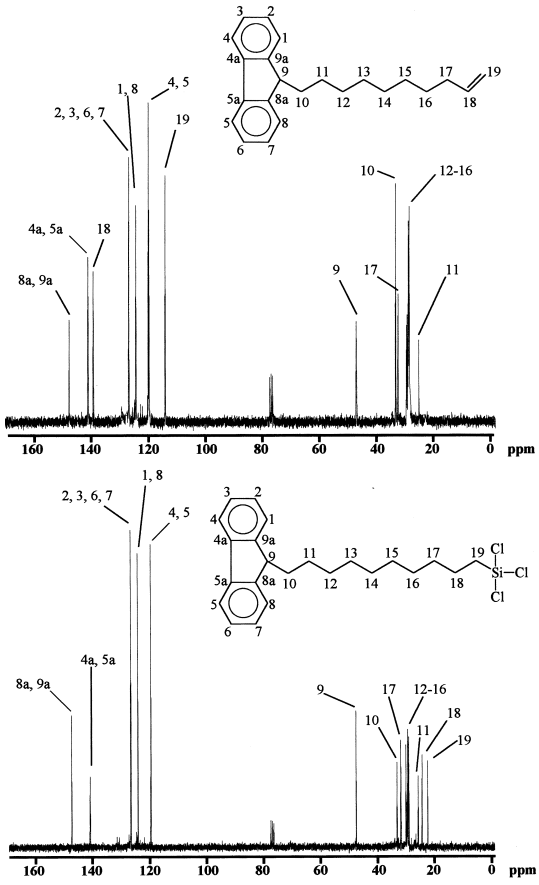

Fig. 1. $^{13}C\{^1H\}$ NMR spectra (62.9 MHz, $CDCl_3$) of **2** and **4a(T^0)**.

*2.6. General procedure for hydrosilation of **1** and **2***

A mixture of the fluorene derivative and the silane was treated with a suspension of hexachloroplatinic

acid in 25 ml of THF and the reaction mixture was stirred for 48 h at 20°C. A dark brown solution was formed and the solvent was removed in vacuo.

2.6.1. 9-(6′-Trichlorosilylhexyl)-9H-fluorene [3a(T^0)]

A 5.7-g (23.0 mmol) amount of **1** was treated with 3 ml (4.023 g, 29.7 mmol) of trichlorosilane and 31.0 mg (0.076 mmol) of hexachloroplatinic acid.

MS (FD) *m/e* 384.2 [M^+, 24], 248.1 [M^+–HCl_3Si, 100]. Anal. Found: C, 58.11; H, 6.45; Cl, 26.01 [27]. $C_{19}H_{21}Cl_3Si$. Calculated: C, 59.46; H, 5.51; Cl, 27.71. $^{13}C\{^1H\}$ NMR (62.90 MHz, $CDCl_3$, 300 K): δ 22.0 (C^{15}), 23.9 (C^{14}), 24.9 (C^{11}), 29.0 (C^{12}), 31.2 (C^{13}), 32.6 (C^{10}), 47.2 (C^9), 119.6 (C^4, C^5), 124.1 (C^1, C^8), 126.7 (C^2, C^7), 126.8 (C^3, C^6), 141.0 (C^{4a}, C^{5a}), 147.2 (C^{8a}, C^{9a}); ^1H NMR (250.13 MHz, $CDCl_3$, 300 K): δ 7.81 (d, ^2J=6.6 Hz, 2H, C^1H, C^8H), 7.57 (d, ^2J=6.9 Hz, 2H, C^4H, C^5H), 7.40 (m, 4H, C^2H, C^3H, C^6H, C^7H), 4.03 (m, 1H, C^9H), 2.05 (m, 2H, $C^{10}H_2$), 1.75 (m, 2H, $C^{11}H_2$), 1.52 (m, 2H, $C^{12}H_2$), 1.31 (m, 6H, $C^{13}H_2$–$C^{15}H_2$).

2.6.2. 9-(6′-Triethoxysilylhexyl)-9H-fluorene [3b(T^0)]

A 10.15-g (40.9 mmol) amount of **1** was treated with 7.7 ml (6.7 g, 40.8 mmol) of triethoxysilane and 13.0 mg (0.032 mmol) of hexachloroplatinic acid.

MS (EI) *m/e* 412.3 [M^+, 10], 250.3 [M^+–$C_6H_{15}O_3Si$,4], 248.1 [M^+–$C_6H_{17}O_3Si$, 23], 177.8 [M^+–$C_{11}H_{25}O_3Si$, 55], 165.1 [M^+–$C_{12}H_{26}O_3Si$, 100]. [27]. $^{13}C\{^1H\}$ NMR (62.90 MHz, $CDCl_3$, 300 K): δ 11.2 (C^{15}), 18.0 ($SiOCH_2\mathit{C}H_3$), 23.6 (C^{14}), 26.6 (C^{11}), 30.4 (C^{12}), 33.2 (C^{13}), 33.4 (C^{10}), 47.0 (C^9), 58.0 ($SiO\mathit{C}H_2CH_3$), 119.5 (C^4, C^5), 123.7 (C^1, C^8), 126.7 (C^2, C^7), 126.8 (C^3, C^6), 140.9 (C^{4a}, C^{5a}), 147.3 (C^{8a}, C^{9a}); ^1H NMR (250.13 MHz, $CDCl_3$, 300 K): δ 7.77 (d, ^2J=7.2 Hz, 2H, C^1H, C^8H), 7.53 (d, ^2J=6.9 Hz, 2H, C^4H, C^5H), 7.35 (m, 4H, C^2H, C^3H, C^6H, C^7H), 3.98 (m, 1H, C^9H), 3.87 (m, 6H, $SiOC\mathit{H}_2CH_3$), 2.02 (m, 2H, $C^{10}H_2$), 1.66 (m, 2H, $C^{11}H_2$), 1.31 (m, 15H, $C^{13}H_2$–$C^{15}H_2$, $SiOCH_2C\mathit{H}_3$), 0.67 (m, 2H, $C^{15}H_2$).

2.6.3. 9-(10′-Trichlorosilyldecyl)-9H-fluorene [4a(T^0)]

A 5.62-g (18.45 mmol) amount of **2** was treated with 1.92 ml (2.57 g, 19.0 mmol) of trichlorosilane and 22.0 mg (0.054 mmol) of hexachloroplatinic acid. The yield was 7.54 g (92.9%).

MS (FD) *m/e* 437.9 [M^+, 16], 304.1 [M^+–HCl_3Si, 100]. Anal. Found: C, 64.31; H, 6.80; Cl, 23.78 [27]. $C_{23}H_{29}Cl_3Si$. Calculated: C, 62.80; H, 6.64; Cl, 24.18. $^{13}C\{^1H\}$ NMR (62.90 MHz, $CDCl_3$, 300 K): δ 22.2 (C^{19}), 24.2 (C^{18}), 25.6 (C^{11}), 28.0 (C^{16}), 29.2 (C^{15}), 29.3 (C^{14}), 29.5 (C^{13}), 29.9 (C^{12}), 31.7 (C^{17}), 33.0 (C^{10}), 47.4 (C^9), 119.7 (C^4, C^5), 124.3 (C^1, C^8), 126.7 (C^2, C^7), 126.8 (C^3, C^6), 141.1 (C^{4a}, C^{5a}), 147.5 (C^{8a}, C^{9a}); ^1H NMR (250.13 MHz, $CDCl_3$, 300 K): δ 7.76 (d, ^2J=7.8 Hz, 2H, C^1H, C^8H), 7.52 (d, ^2J=6.9 Hz, 2H, C^4H, C^5H), 7.34 (m, 4H, C^2H, C^3H, C^6H, C^7H), 3.98 (t, ^2J=6.0 Hz, 1H, C^9H), 2.02 (m, 2H, $C^{10}H_2$), 1.56 (m, 2H, $C^{19}H_2$), 1.41 (m, 2H, $C^{18}H_2$), 1.37 (m, 2H, $C^{17}H_2$), 1.24 (m, 12H, $C^{11}H_2$–$C^{16}H_2$).

2.6.4. 9-(10′-Triethoxysilyldecyl)-9H-fluorene [4b(T^0)]

A 4.35-g (14.30 mmol) amount of **2** was treated with 2.68 ml (2.35 g, 14.30 mmol) of triethoxysilane and 19.0 mg (0.046 mmol) of hexachloroplatinic acid.

MS (FD) *m/e* 468.1 [M^+, 6], 304.1 [M^+–$C_6H_{15}O_3Si$, 100] [27]. $^{13}C\{^1H\}$ NMR (62.90 MHz, $CDCl_3$, 300 K): δ 14.0 (C^{19}), 18.2 ($SiOCH_2\mathit{C}H_3$), 22.7 (C^{18}), 25.6 (C^{11}), 29.0 (C^{16}), 29.2 (C^{15}), 29.3 (C^{14}), 29.5 (C^{13}), 29.9 (C^{12}), 32.5 (C^{17}), 33.0 (C^{10}), 47.4 (C^9), 59.1 ($SiO\mathit{C}H_2CH_3$), 119.6 (C^4, C^5), 124.2 (C^1, C^8), 126.6 (C^2, C^7), 126.7 (C^3, C^6), 141.0 (C^{4a}, C^{5a}), 147.5 (C^{8a}, C^{9a}); ^1H NMR (250.13 MHz, $CDCl_3$, 300 K): δ 7.72 (d, ^2J=6.9 Hz, 2H, C^1H, C^8H), 7.60 (d, ^2J=6.9 Hz, 2H, C^4H, C^5H), 7.30 (m, 4H, C^2H, C^3H, C^6H, C^7H), 3.94 (m, 7H, $SiOC\mathit{H}_2CH_3$, C^9H), 1.96 (m, 2H, $C^{10}H_2$), 1.61 (m, 2H, $C^{11}H_2$), 1.24 (m, 18H, $C^{12}H_2$–$C^{18}H_2$), 1.20 (m, 9H, $SiOCH_2C\mathit{H}_3$), 0.63 (m, 2H, $C^{19}H_2$).

2.6.5. 9-(10′-Chlorodimethylsilyldecyl)-9H-fluorene [4c(M^0)]

A 5.31-g (17.44 mmol) amount of **2** was treated with 1.96 ml (1.70 g, 18.00 mmol) of chlorodimethylsilane and 17.0 mg (0.041 mmol) of hexachloroplatinic acid. The yield was 6.80 g (97.7%).

MS (FD) *m/e* 398.1 [M^+, 84], 303.9 [M^+–C_2H_7ClSi, 100]. Anal. Found:. C, 75.67; H, 8.97; Cl,

9.03. $C_{25}H_{35}ClSi$. Calculated: C, 75.24; H, 8.84; Cl, 8.88. $^{13}C\{^1H\}$ NMR (62.90 MHz, $CDCl_3$, 300 K): δ 1.6 ($SiCH_3$), 18.9 (C^{19}), 22.9 (C^{18}), 25.6 (C^{11}), 29.2 (C^{16}), 29.35 (C^{15}), 29.41 (C^{14}), 29.6 (C^{13}), 29.9 (C^{12}), 32.0 (C^{17}), 33.0 (C^{10}), 47.4 (C^9), 119.7 (C^4, C^5), 124.3 (C^1, C^8), 126.7 (C^2, C^7), 126.8 (C^3, C^6), 141.0 (C^{4a}, C^{5a}), 147.5 (C^{8a}, C^{9a}); ^1H NMR (250.13 MHz, $CDCl_3$, 300 K): δ 7.62 (d, ^2J=7.5 Hz, 2H, C^1H, C^8H), 7.38 (d, ^2J=6.9 Hz, 2H, C^4H, C^5H), 7.20 (m, 4H, C^2H, C^3H, C^6H, C^7H), 3.84 (t, ^2J =5.7 Hz, 1H, C^9H), 1.88 (m, 2H, $C^{10}H_2$), 1.16 (m, 2H, $C^{18}H_2$), 1.09 (m, 14H, $C^{11}H_2$–$C^{17}H_2$), 0.69 (s, 2H, $C^{19}H_2$), 0.27 (m, 6H, $SiCH_3$).

2.7. Preparation of the fluorene phases [3b(T^n)(Q^m)$_y$] and [4b(T^n)(Q^m)$_y$] [33]

A 5-g amount of silica (with about 50% from a total of 8 μmol/m^2 of reactive surface hydroxy groups) was dried under vacuum conditions at 180°C for 4 h. After cooling to 120°C, the flask was aerated and a threefold molar excess of ethoxysilane was added, without any addition of solvent. The flask was equipped with a frit (G4) and a drying tube, and the mixture was heated to 120°C for another 12 h. The product was filtered off, washed twice with 40 ml of toluene, methanol and petroleum ether and, finally, the product was vacuum dried at 60°C for 1 h.

2.8. Preparation of the fluorene phases [3a(T^n)(Q^m)$_y$], [4a(T^n)(Q^m)$_y$] and [4c(M^1)(Q^m)$_y$]

A 5-g amount of silica (with about 50% from a total of 8 μmol/m^2 of reactive surface hydoxy groups) was dried under vacuum conditions at 180°C for 4 h. After cooling to 70°C, the flask was aerated and the silica was suspended in 20 ml of toluene. Then, a threefold molar excess of chlorosilane was added and the solution was stirred for 15 min. To induce the silanization reaction, 1 ml of water was added and the solution was refluxed at 120°C for another 18 h. For monochlorosilanes, 1 ml of 2,6-lutidine was added instead of water. The product was filtered off, washed twice with 40 ml of toluene, methanol and petroleum ether and, finally, the product was vacuum dried at 60°C for 1 h.

3. Results and discussion

3.1. Synthesis

The introduction of alkyl chains in the 9-position of the fluorene molecule can be easily performed by a reaction of the fluorenyl anion with alkyl bromides [34–36]. In the presence of additional functional groups at the alkyl chain, problems may occur, because these groups are sensitive to moisture. In the present case, it was not possible to introduce a chlorosilyl group at the alkyl chain, because an immediate polymerization of the silyl groups takes place. Therefore, in a first step, 5′-hexenyl and 9′-decenyl substituents were introduced at the 9-position of fluorene and, subsequently, the hydrosilation of the terminal double bonds was carried out (Scheme 1).

The 9-(5′-hexenyl)-9*H*- and 9-(9′-decenyl)-9*H*-fluorenes (**1** and **2**) are obtained as highly viscous yellow oils that have two characteristic singlets at 114.2 and 139.0 ppm, indicating terminal double bonds, in their $^{13}C\{^1H\}$ NMR spectra ($CDCl_3$). In the ^1H NMR spectra of **1** and **2**, the signal of the proton in the 9-position is split into a triplet, due to coupling with the adjacent methylene protons ($C^{10}H_2$).

Hydrosilation of **1** and **2** was performed with different hydrosilanes to control the coverage density of silica-bound phases (Table 1). Hence, **1** was hydrosilated with trichlorosilane and triethoxysilane, using hexachloroplatinic acid as a catalyst. When trichlorosilane was used, 9-(6′-trichlorosilylhexyl)-9*H*-fluorene [**3a(T^0)**] was obtained in good yield. The $^{13}C\{^1H\}$ NMR spectrum of **3a(T^0)** reveals two signals at 22.0 and 23.9 ppm, which is in agreement with the two terminal methylene groups of the hexyl spacer. The alternative reaction between **1** and triethoxysilane leads only to approximately a 50% conversion [32].

The reaction of **2** with different silanes showed similar results. With trichlorosilane was used, 9-(10′-trichlorosilyldecyl)-9*H*-fluorene [**4a(T^0)**] was obtained in good yield. In Fig. 1, both $^{13}C\{^1H\}$ NMR spectra of **2** and **4a(T^0)** are displayed. As in the example of **1** and **3a(T^0)**, the success of the completion of the reaction could be monitored by the

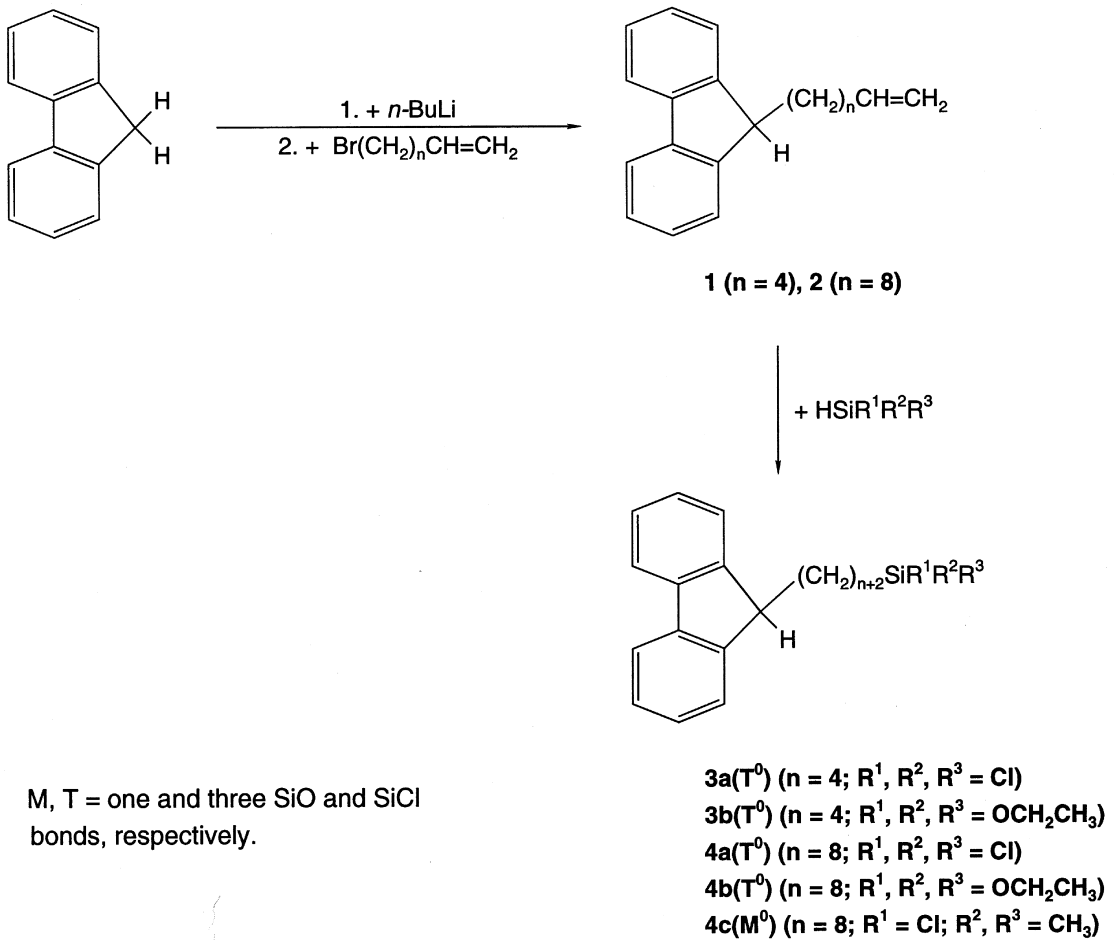

Scheme 1.

disappearance of the $^{13}C\{^1H\}$ signals that were due to the original terminal alkenyl groups.

In a further hydrosilation experiment of **2** with chlorodimethylsilane, 9-(10′-chloro-dimethylsilyl-decyl)-9*H*-fluorene [**4c(M^0)**] was isolated. In the $^{13}C\{^1H\}$ NMR spectrum of **4c(M^0)**, two signals at 18.9 and 22.9 ppm occur, both indicating terminal methylene groups. Another resonance at 1.6 ppm is attributed to the $Si(CH_3)_2$ groups. In an analogy to the hydrosilation of **1** with triethoxysilane, only a 50% yield of 9-(10′-triethoxysilyldecyl)-9*H*-fluorene [**4b(T^0)**] could be achieved using **2** as an educt [37].

Table 1
ω-Silylalkyl fluorenes

Educt	$SiCl_3$	$Si(OCH_2CH_3)_3$	$SiCl(CH_3)_2$
9-(5′-Hexenyl)-9*H*-fluorene (**1**, *n*=6)	**3a(T^0)**	**3b(T^0)**	
9-(9′-Decenyl)-9*H*-fluorene (**2**, *n*=10)	**4a(T^0)**	**4b(T^0)**	**4c(M^0)**

The observation of different reactivities of the employed hydrosilanes, e.g. trichlorosilane, chlorodimethylsilane and triethoxysilane, is in agreement with the investigations of Capka et al. [38], who observed a significant increase in the reactivity of hydrosilanes towards 1-heptene with a growing number of chlorine atoms. This phenomenon is ascribed to the increase in the polarity at the silicon–hydrogen bond caused by successive replacement of methyl or ethoxy groups by the more electronegative chlorine atoms.

Finally, each of the five synthesized fluorenyl alkyl silanes was immobilized on silica gel with a particle size of 5 μm and an average pore diameter of 200 Å. The resulting new stationary phases are depicted in Fig. 2. Independent of the length of the alkyl spacer, a much higher ligand density [39] could be secured by the use of trichlorosilanes instead of triethoxysilanes. The ligand densities of the phases fluorene-6B [**3b(T^n)(Q^m)$_y$**] [40] (1.24 μmol/m^2) and fluorene-10B [**4b(T^n)(Q^m)$_y$**] (0.9 μmol/m^2) were much lower than those of the phases fluorene-6A [**3a(T^n)(Q^m)$_y$**] (3.98 μmol/m^2) and fluorene-10A [**4a(T^n)(Q^m)$_y$**] (3.69 μmol/m^2), indicating a much higher reactivity of the respective trichlorosilane. The ligand density of the monofunctional phase fluorene-10C [**4c(T^n)(Q^m)$_y$**] (1.77 μmol/m^2) is even higher than that of trifunctional phases in which triethoxysilanes were used. For further characterization of the new stationary phases, solid-state NMR spectroscopy is the method of choice.

3.2. Characterization by solid-state NMR spectroscopy

Information about the surface of the silica gel prior to and after immobilization of the fluorenyl alkyl silanes is available by ^{29}Si CP/MAS NMR spectroscopy [41]. Unmodified silica gel consists of three main surface species, which can be clearly identified. The characteristic NMR signals of silanediol groups (Q^2), silanol groups (Q^3) and siloxane groups (Q^4) appear at −92, −101 and −110 ppm, respectively [16,42].

Depending on the functionality of the added silanes [**3a(T^0)**], [**3b(T^0)**] and [**4a(T^0)**]–[**4c(M^0)**] (Scheme 1), additional characteristic NMR reso-

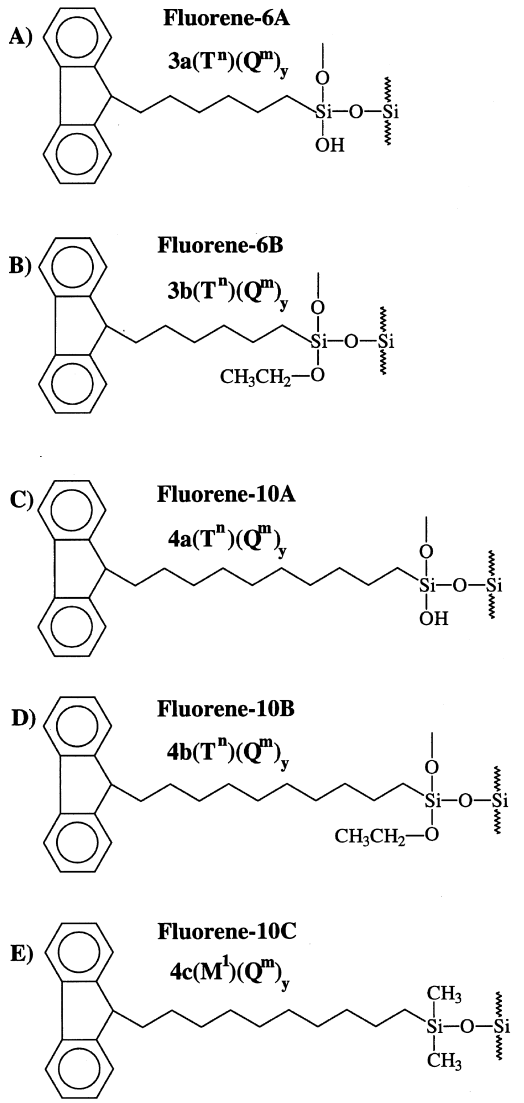

Fig. 2. Each of the five new stationary phases consists of silica gel with a particle size of 5 μm and an average pore diameter of 200 Å. (A) Stationary phase, fluorene-6A **[3a(T^n)(Q^m)$_y$]** was prepared using 9-(6′-trichlorosilylhexyl)-9*H*-fluorene **[3a(T^0)]**, the ligand density of chemically bound fluorene is 3.98 μmol/m^2. (B) Stationary phase, fluorene-6B **[3b(T^n)(Q^m)$_y$]**; used silane: 9-(6′-triethoxysilylhexyl)-9*H*-fluorene **[3b(T^0)]**; ligand density, 1.24 μmol/m^2. (C) Stationary phase, fluorene-10A **[4a(T^n)(Q^m)$_y$]**; used silane: 9-(10′-trichlorosilyldecyl)-9*H*-fluorene **[4a(T^0)]**; ligand density, 3.69 μmol/m^2. (D) Stationary phase, fluorene-10B **[4b(T^n)(Q^m)$_y$]**; used silane: 9-(10′-triethoxysilyldecyl)-9*H*-fluorene **[4b(T^0)]**; ligand density, 0.9 μmol/m^2. (E) Stationary phase, fluorene-10C **[4c(M^1)(Q^m)$_y$]**; used silane: 9-(10′-chlorodimethylsilyldecyl)-9*H*-fluorene **[4c(M^0)]**; ligand density, 1.77 μmol/m^2.

nances occur after their immobilization on the silica gel surface [11,16]. Fig. 3 shows the ^{29}Si CP/MAS NMR spectra of the two stationary phases, fluorene-10C [**4c(M^1)(Q^m)$_y$**] and fluorene-6A [**3a(T^n)(Q^m)$_y$**]. The monofunctionality of the phase fluorene-10C [**4c(M^1)(Q^m)$_y$**] is clearly proved by the appearance of the M group singlet at 13 ppm (Fig. 3 A), whereas the T group resonances of trifunctional silanes are detected in a chemical shift region between −48 and −66 ppm. In the spectrum of the phase fluorene-6A [**3a(T^n)(Q^m)$_y$**] (Fig. 3B), only the T^2 and T^3 group signals are perceptible at −58 and −66 ppm, respectively. The absence of a T^1 signal at −48 ppm indicates that there is a higher degree of crosslinking between the immobilized silanes on the silica gel surface. Determination of the exact degree of crosslinking is performed by peak deconvolution of the T group signals. A comparison of the intensity of the deconvoluted peaks is possible because of the approximately same crosspolarization characteristics of the investigated T species. The highest degree of crosslinking (Q) was calculated [16] for the phase fluorene-6A [**3a(T^n)(Q^m)$_y$**] (Q=85.2%), which was followed by the phases fluorene-10A [**4a(T^n)(Q^m)$_y$**] (Q=82.4%), fluorene-10B [**4b(T^n)(Q^m)$_y$**] (Q=69.1%) and fluorene-6B [**3b(T^n)(Q^m)$_y$**] (Q=66.9%). Because of the employment of $HSiCl_3$ instead of $HSi(OCH_2CH_3)_3$, the fluorenyl alkyl silanes show a much higher degree of crosslinking on the silica gel surface, which corresponds to a higher ligand density.

^{13}C CP/MAS NMR spectroscopy provides information about the structure of the immobilized organic ligand fragments [24,43,44]. Fig. 4 reveals the ^{13}C CP/MAS NMR spectra of the fluorene phases [**4a(T^n)(Q^m)$_y$**] and [**4b(T^n)(Q^m)$_y$**]. The spectrum of the phase fluorene-10A [**4a(T^n)(Q^m)$_y$**] (3.69 μmol/m^2; Fig. 4A) has a much better signal-to-noise ratio, due to the higher ligand density compared to the spectrum of the phase fluorene-10B [**4b(T^n)(Q^m)$_y$**]

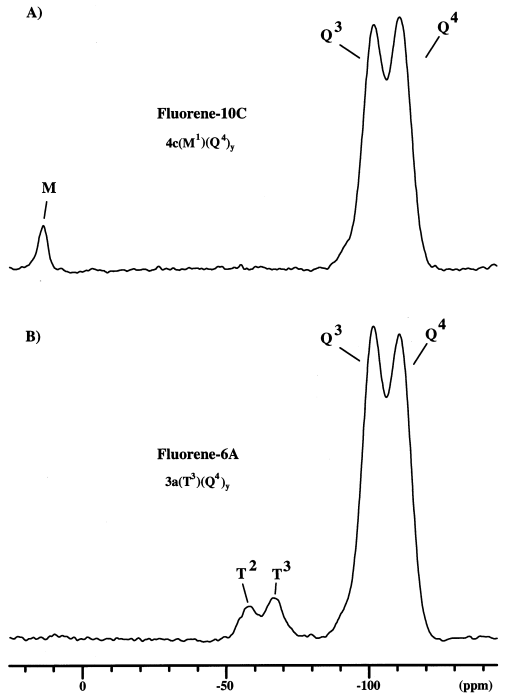

Fig. 3. ^{29}Si-CP/MAS NMR spectra (rf, 3000 Hz) of the stationary phases fluorene-10C **[4c(M^1)(Q^m)$_y$]** (A) and fluorene-6A **[3a(T^n)(Q^m)$_y$]** (B). The different functionalities of the silanes are clearly recognizable. The lower the functionality of the silane, the greater the low field shift of the signals is after the immobilization on the silica gel surface.

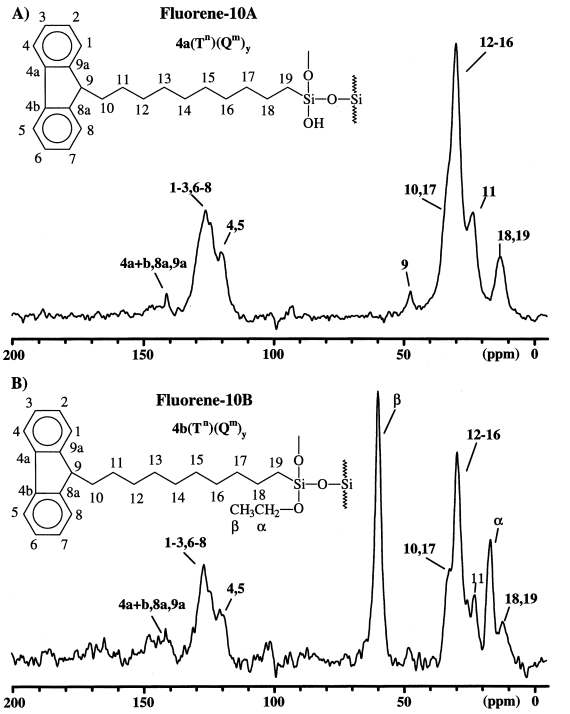

Fig. 4. ^{13}C CP/MAS NMR spectra (rf, 10000 Hz) of the stationary phases fluorene-10A **[4a(T^n)(Q^m)$_y$]** and fluorene-10B **[4b(T^n)(Q^m)$_y$]**.

(0.9 μmol/m^2; Fig. 4B), in which C^9 is barely detectable. Furthermore, the spectrum in Fig. 4B is dominated by the signals of the unconverted ethoxy groups of the employed silane at 60 ppm and 17 ppm, respectively. This observation agrees well with the calculated lower degree of crosslinking obtained by peak deconvolution of the T group signals from the ^{29}Si CP/MAS NMR spectra, indicating a lower reactivity of triethoxysilanes compared to trichlorosilanes. If the ^{13}C solid-state NMR spectrum of fluorene-10A [**4a(T^n)(Q^m)$_y$**] (Fig. 4A) is compared with the high resolution ^{13}C NMR spectrum of the corresponding fluorenyl alkyl silane **4a(T^0)** in $CDCl_3$ (Fig. 1), the high field shift of the spacer atoms C^{18} and C^{19} is identifiable. This is due to the absence of the chlorine atoms after immobilization of the silane. All other chemical shifts do not differ significantly between the spectra measured in solution and in the solid-state. The resonances in the solid-state spectrum are broadened, due to the tethering of the molecules to the silica gel. Therefore, the signals of the different aromatic carbon atoms are not resolved. The low intensity of the quaternary aromatic carbon atoms can be explained by the absence of adjacent protons, but the weak crosspolarization efficiency is also an indication for an improved mobility of the fluorene ligand fragment [10].

The method of ^{1}H MAS NMR spectroscopy also provides valuable information about the organic ligand moieties attached on the silica gel surface. Usually, strong homonuclear dipole–dipole interactions cause signal line widths of up to 30–40 kHz in solid-state ^{1}H MAS NMR spectra. However, in systems with diluted protons, such as the new fluorene phases, the strong homonuclear dipole–dipole interactions can be drastically reduced simply by employing high rotational frequencies, up to 14 kHz [16,45–47]. Using this method, well resolved ^{1}H MAS NMR spectra can be obtained.

The ^{1}H MAS NMR spectrum of fluorene-10C [**4c(M^1)(Q^m)$_y$**] is depicted in Fig. 5. It demonstrates three well-resolved main peaks. One of the alkyl spacer protons at 1.2 ppm also includes a shoulder at 0 ppm for the methyl protons of the monofunctional silane. The remaining surface hydroxy groups of the silica gel and the fluorene proton in the 9-position are responsible for the signal at 3.9 ppm, whereas the aromatic fluorene protons are detected by a separate

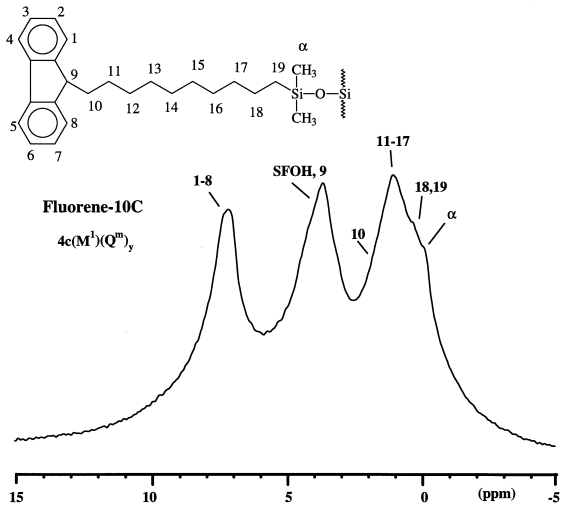

Fig. 5. ^{1}H MAS spectrum (rf, 14000 Hz) of the stationary phase fluorene-10C **[4c(M^1)(Q^m)$_y$]** at 295 K. A higher overall mobility is indicated by a rather small signal of the aromatic protons. The remaining surface hydroxy groups of the silica gel are marked as SFOH, their signal is overlapping with that of the fluorene proton in the 9-position.

signal at 7 ppm. Compared to other stationary phases containing aromatic ligand fragments [11], in this case, the signal of the aromatic protons has a very small line width and is well separated from the other signals. This points to an overall higher mobility of the stationary phase fluorene-10C [**4c(M^1)(Q^m)$_y$**].

3.3. HPLC application

The separation efficiency of the new fluorene phases [**3a(T^n)(Q^m)$_y$**], [**3b(T^n)(Q^m)$_y$**], [**4a(T^n)(Q^m)$_y$**], [**4b(T^n)(Q^m)$_y$**] and [**4c(M^1)(Q^m)$_y$**] was investigated using the Sander and Wise test (SRM 869) [2,26]. Originally, this test was used for the characterization of *n*-alkyl stationary phases. Depending on the relative elution order of the three test compounds, BaP (benzo[*a*]pyrene), PhPh (phenanthro[3,4-*c*]phenanthrene) and TBN (tetrabenzonaphthalene), *n*-alkyl phases are classified as polymeric ($\alpha_{TBN/BaP}<1.0$), intermediate ($1.0<\alpha_{TBN/BaP}<1.7$), or monomeric ($\alpha_{TBN/BaP}>1.7$). In the case of the fluorenyl alkyl phases, this classification cannot be applied, because π–π interactions dominate the separation process instead of hydrophobic interac-

tions. In particular, due to these π–π interactions [10,13], the different fluorene phases should be qualified to separate the mixture of the three PAHs, demonstrating their usefulness for HPLC separations.

In Table 2, the retention times of the test samples are summarized, using the five new fluorene phases (Fig. 2). For the phases with a decyl spacer ([**4a(T^n)(Q^m)$_y$**], [**4b(T^n)(Q^m)$_y$**] and [**4c(M^1)(Q^m)$_y$**]), PhPh is eluted prior to BaP, followed by TBN, whereas this elution order is changed by the use of fluorene phases with a hexyl spacer ([**3a(T^n)(Q^m)$_y$**] and [**3b(T^n)(Q^m)$_y$**]). In the present case, BaP eluted first, followed by PhPh and, finally, TBN. The change in the elution order, which is due to a different alkyl spacer length, is illustrated in Fig. 6.

Another important fact is the correlation of the retention times with the degree of ligand density of the respective fluorene phases. The higher the amount of chemically bound fluorene, the longer are the retention times of the solute molecules. This is consistent with an increased π–π interaction, because the selectivity of the $\alpha_{TBN/BaP}$ value is not influenced much by either a different functionality of the used silane or by the ligand density for phases with the same alkyl spacer length. By ^{29}Si CP/MAS NMR spectroscopy, a much higher degree of cross-linking was determined for fluorene-10A [**4a(T^n)(Q^m)$_y$**] than for the phase fluorene-10B [**4b(T^n)(Q^m)$_y$**]. By ^{13}C CP/MAS NMR spectroscopy, a high amount of unconverted ethoxy groups was also detected for the second phase. However, the $\alpha_{TBN/BaP}$ value for fluorene-10B [**4b(T^n)(Q^m)$_y$**] with a rather low ligand density (0.9 μmol/m^2) is smaller than the $\alpha_{TBN/BaP}$ value of fluorene-10A [**4a(T^n)(Q^m)$_y$**] with a very high ligand density (3.69 μmol/m^2). Furthermore, the large amount of unconverted ethoxy groups may lead to long-term differences in the chromatographic behavior, due to hydrolysis caused by the use of acetonitrile–water mixtures. In terms of *n*-alkyl phases, fluorene-10B [**4b(T^n)(Q^m)$_y$**] would be classified as being more polymeric than fluorene-10A [**4a(T^n)(Q^m)$_y$**]. However, this is in marked contrast to the results obtained by the different solid-state NMR techniques. Additionally, ^{29}Si CP/MAS NMR spectroscopy is able to identify fluorene-10C [**4c(M^1)(Q^m)$_y$**] as a typical monomeric phase by detection of the strong M group

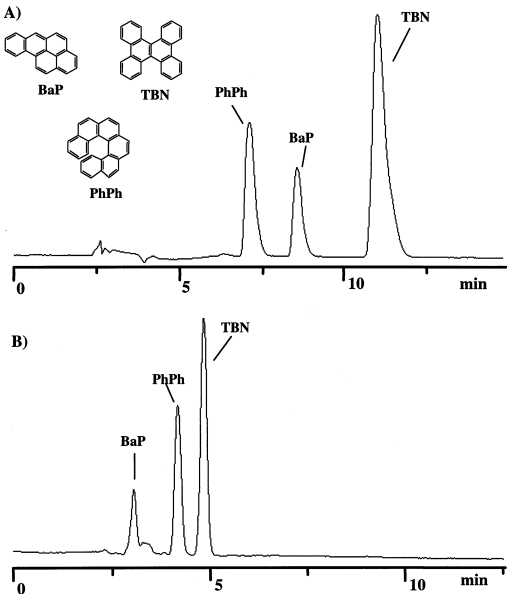

Fig. 6. Comparison of the elution order of the SRM 869 test sample by use of stationary phases with different spacer lengths. (A) stationary phase, fluorene-10A **[4a(T^n)(Q^m)$_y$]**. (B) stationary phase, fluorene-6B **[3b(T^n)(Q^m)$_y$]**. Conditions in both cases were as follows: Mobile phase, acetonitrile–water (85:15, v/v); temperature, 25°C; wavelength, 254 nm; flow-rate, 1 ml/min.

Table 2
Retention times, t' (min) of the SRM 869 test components applied on the different fluorene phases

Stationary phase	t'(BaP)	t'(PhPh)	t'(TBN)	$\alpha_{TBN/BaP}$	Ligand density (μmol/m^2)
Fluorene-6A [**3a(T^n)(Q^m)$_y$**]	4.00	4.39	7.25	1.81	3.98
Fluorene-6B [**3b(T^n)Q^m)$_y$**]	0.74	1.87	2.63	3.55	1.24
Fluorene-10A [**4a(T^n)(Q^m)$_y$**]	5.92	4.47	8.34	1.41	3.69
Fluorene-10B [**4b(T^n)(Q^m)$_y$**]	1.22	0.53	1.66	1.36	0.9
Fluorene-10C [**4c(M^1)(Q^m)$_y$**]	4.20	3.86	6.69	1.59	1.77

The selectivity $\alpha_{TBN/BaP}$ and the ligand density (μmol/m^2) of the respective fluorene phases provide further information about their separation efficiencies.

signal at 13 ppm (Fig. 3). However, the $\alpha_{TBN/BaP}$ value of **4c(M^1)(Q^m)$_y$** is below 1.7, pointing to an intermediate phase in terms of *n*-alkyl phases. Both fluorene phases with a hexyl spacer have $\alpha_{TBN/BaP}$ values larger than 1.7. In contrast to that finding, ^{29}Si CP/MAS NMR measurements identified them as being polymeric, especially in the case of fluorene-6A [**3a(T^n)(Q^m)$_y$**], which reveals strong T group resonances and the highest degree of crosslinking (Fig. 3). The $\alpha_{TBN/BaP}$ value of fluorene-6B [**3b(T^n)(Q^m)$_y$**] is extremely high, but it has approximately the same degree of crosslinking and an even higher ligand density than the phase fluorene-10B [**4b(T^n)(Q^m)$_y$**], which has the lowest $\alpha_{TBN/BaP}$ value of all of the fluorene phases investigated.

4. Conclusion

For the first time, stationary phases were synthesized in which fluorene was attached on the silica gel surface by *n*-alkyl spacers. Solid-state NMR spectroscopy was able to characterize the structure of these fluorene phases and proved a much higher reactivity of the employed trichlorosilanes compared to the respective triethoxysilanes. In addition, a higher mobility of the fluorene ligand fragments was indicated by this technique. The utility of the new fluorene phases [**3a(T^n)(Q^m)$_y$**], [**3b(T^n)(Q^m)$_y$**], [**4a(T^n)(Q^m)$_y$**], [**4b(T^n)(Q^m)$_y$**] and [**4c(M^1)(Q^m)$_y$**] was demonstrated by using the Sander and Wise test (SRM 869). The results obtained corroborate the finding that the fluorene phases cannot be classified in the same way as *n*-alkyl phases. Furthermore, their retention behavior points to the existence of a different interaction mechanism. The retention times of the sample molecules depend on the amount of chemically bound fluorene, whereas the functionality of the employed silanes does not influence the elution order significantly, in contrast to that of *n*-alkyl phases.

A detailed characterization of the dynamic behavior of these newly developed fluorene phases by solid-state NMR spectroscopy and further HPLC applications will be described in part II of these investigations.

Acknowledgements

We wish to thank Bischoff Analysentechnik und -geräte GmbH (Leonberg, Germany) for providing silica gel, and Dr. Rainer Brindle and Brigitte Schindler for their support in performing solid-state NMR measurements. Dr. Lane C. Sander (NIST, Gaithersburg, USA) is thanked for the donation of the SRM 869 test mixture. Financial support by the Deutsche Forschungsgemeinschaft (Forschergruppe, grant No. Li 154/41-3) is gratefully acknowledged.

References

[1] K.K. Unger (Editor), Chromatogr. Sci., Vol. 47 (Packings and Stationary Phases in Chromatographic Techniques), Marcel Dekker, New York, Basel, 1990.
[2] L.C. Sander, S.A. Wise, in R.M. Smith (Editor), Retention and Selectivity in Liquid Chromatography (Journal of Chromatography Library, Vol. 57), Elsevier, Amsterdam, 1995, p. 337.
[3] F. Mikes, G. Boshart, E. Gil-Av, J. Chem. Soc. Chem. Commun., (1976) 99.
[4] F. Mikes, G. Boshart, E. Gil-Av, J. Chromatogr., 122 (1976) 205.
[5] N. Tanaka, Y. Tokuda, K. Iwaguchi, M. Araki, J. Chromatogr., 239 (1982) 761.
[6] C.H. Lochmüller, M.L. Hunnicutt, R.W. Beaver, J. Chromatogr. Sci., 21 (1983) 444.
[7] M. Verzele, N. van de Velde, Chromatographia, 20 (1985) 239.
[8] M. Diack, R.N. Compton, G. Guiochon, J. Chromatogr., 639 (1993) 129.
[9] M. Funk, H. Frank, F. Oesch, K.L. Platt, J. Chromatogr. A, 659 (1994) 57.
[10] R. Brindle, K. Albert, J. Chromatogr. A, 757 (1997) 3.
[11] A. Ellwanger, R. Brindle, K. Albert, J. High Resolut. Chromatogr., 20 (1997) 39.
[12] H.-J. Egelhaaf, D. Oelkrug, A. Ellwanger, K. Albert, J. High Resolut. Chromatogr., in press.
[13] H. Hemetsberger, in K. K. Unger (Editor), Chromatogr. Sci., Vol. 47 (Packings and Stationary Phases in Chromatographic Techniques), Marcel Dekker, New York, Basel, 1990, p. 511.
[14] A. Tchapla, S. Heron, E. Lesellier, H. Colin, J. Chromatogr. A, 656 (1993) 81.
[15] J.G. Dorsey, K.A. Dill, Chem. Rev., 89 (1989) 331.
[16] M. Pursch, S. Strohschein, H. Händel, K. Albert, Anal. Chem., 68 (1996) 386.
[17] F.R. Hartley, Supported Metal Complexes, D. Reidel, Boston, MA, 1985.
[18] U. Deschler, P. Kleinschmit, P. Panster, Angew. Chem., Int. Ed. Engl., 25 (1986) 236.

[19] E. Lindner, M. Kemmler, H.A. Mayer, P. Wegner, J. Am. Chem. Soc., 116 (1994) 348.
[20] E. Lindner, M. Kemmler, T. Schneller, H.A. Mayer, Inorg. Chem., 34 (1995) 5489.
[21] E. Lindner, A. Jäger, T. Schneller, H.A. Mayer, Chem. Mater., 9 (1997) 81.
[22] E. Lindner, A. Jäger, M. Kemmler, F. Auer, P. Wegner, H.A. Mayer, A. Benez, E. Plies, Inorg. Chem., 36 (1997) 862.
[23] E.S.P. Bouvier, S.A. Oehrle, LC·GC Int., 8 (1995) 338.
[24] K. Albert, E. Bayer, J. Chromatogr., 544 (1991) 345.
[25] C.A. Fyfe (Editor), Solid State NMR for Chemists, C.F.C. Press, Guelph, Ontario, 1983.
[26] L.C. Sander, J. Chromatogr. Sci., 26 (1988) 380.
[27] L.C. Sander, S.A. Wise, LC·GC Int., 3 (1990) 24.
[28] W. Schöniger, Microchim. Acta, (1955) 123.
[29] A. Dirschel, F. Erne, Microchim. Acta (1961) 866.
[30] C.K. Narula, K.T. Mak, R.F. Heck, J. Org. Chem., 48 (1983) 2792.
[31] A. Singh, M.A. Markowitz, New J. Chem., 18 (1994) 377.
[32] Due to the incomplete hydrosilation reaction no satisfactory elemental analyses were obtainable. Because of the still present educt, the carbon value was found to be too high, whereas the hydrogen value was too low.
[33] J. Schmid, K. Albert, E. Bayer, J. Chromatogr. A, 694 (1995) 333.
[34] K. Albert, A. Rieker, Chem. Ber., 110 (1977) 1804.
[35] S. Gronert, A. Streitwieser, J. Amer. Chem. Soc., 110 (1988) 2836.
[36] K. Patsidis, H.G. Alt, J. Organomet. Chem., 501 (1995) 31.
[37] Nevertheless, the existence of the hydrosilated products could be proved by FD-MS. In the $^{13}C\{^{1}H\}$ NMR spectra of **3b(T^0)** and **4b(T^0)**, two signals in the alkyl area are attributed to the terminal methylene groups of the spacer. Due to the sensitivity of the silyl group to moisture, purification of these compounds proved to be difficult. However, further purification is not necessary because the educts **1** and **2** are washed out during the modification process.
[38] M. Capka, P. Svoboda, V. Bazant, V. Chvalovsky, Coll. Czech. Chem. Commun., 36 (1971) 2785.
[39] B. Buszewski, Chromatographia, 34 (1992) 573.
[40] M, T, Q=one, two and three SiO and SiCl bonds, respectively; n=0–3, m=0–4.
[41] G.E. Maciel, D.W. Sindorf, J. Am. Chem. Soc., 102 (1980) 7606.
[42] E. Bayer, K. Albert, J. Reiners, M. Nieder, D. Müller, J. Chromatogr., 264 (1983) 197.
[43] M. Pursch, R. Brindle, A. Ellwanger, L.C. Sander, C.M. Bell, H. Händel, K. Albert, Solid-State NMR, in press.
[44] J.J. Pesek, M.T. Matyska, J. Ramakrishnan, Chromatographia, 44 (1997) 538.
[45] S.F. Dec, C.E. Bronnimann, R.A. Wind, G.E. Maciel, J. Magn. Reson., 82 (1989) 454.
[46] R. Brindle, M. Pursch, K. Albert, Solid-State NMR, 6 (1996) 251.
[47] M. Pursch, L. Sander, K. Albert, Anal Chem., 68 (1996) 4107.